Geomechanics and Engineering, *Vol. 33, No. 6 (2023) 611-624*
https://doi.org/10.12989/gae.2023.33.6.611

Predicting unconfined compression strength and split tensile strength of soil-cement via artificial neural networks

Luís Pereira*, Luís Godinho and Fernando G. Branco

University of Coimbra, ISISE, ARISE, Department of Civil Engineering, Coimbra, Portugal

(*Received March 24, 2022, Revised May 9, 2023, Accepted May 11, 2023*)

Abstract. Soil properties make it attractive as a building material due to its mechanical strength, aesthetically appearance, plasticity, and low cost. However, it is frequently necessary to improve and stabilize the soil mechanical properties with binders. Soil-cement is applied for purposes ranging from housing to dams, roads and foundations. Unconfined compression strength (UCS) and split tensile strength (CD) are essential mechanical parameters for ascertaining the aptitude of soil-cement for a given application. However, quantifying these parameters requires specimen preparation, testing, and several weeks. Methodologies that allowed accurate estimation of mechanical parameters in shorter time would represent an important advance in order to ensure shorter deliverable timeline and reduce the amount of laboratory work. In this work, an extensive campaign of UCS and CD tests was carried out in a sandy soil from the Leiria region (Portugal). Then, using the machine learning tool *Neural Pattern Recognition* of the MATLAB software, a prediction of these two parameters based on six input parameters was made. The results, especially those obtained with resource to a Bayesian regularization-backpropagation algorithm, are frankly positive, with a forecast success percentage over 90% and very low root mean square error (RMSE).

Keywords: artificial neural networks; compression; flexural; mechanical properties; soil-cement

1. Introduction

The development of modern societies has led to migratory flows towards the biggest population centers, with repercussions on the exponential increase of the urban population. This population density increase has as a direct consequence an increase in the need to carry out all types of construction works to provide accommodation, ease the movement and storage of natural resources to ensure an improved quality of life. The construction of infrastructures in poor geotechnical characteristics soils (low mechanical strength and high compressibility) is frequently possible only by resorting to ingenious and creative ways to improve the performance of these soils, (Erzín and Gul 2013) with chemical stabilization being one of the most successful measures (Correia *et al.* 2013, Ngo *et al.* 2021, Javadi and Rezania 2009). Cement was used for the first time as a soil stabilizer in the construction of a road in Sarasota, Florida (United States of America), in 1915 (Wang 2002).

Nowadays, the use of cement as a soil improvement technique is used worldwide. This technique is used especially in the base and subbase layers, but can also be used in several other applications such as: earth dams slopes, protection of critical areas in watercourse beds with high erosive action, support layer for superficial foundations (Luat *et al.* 2020) prevention of soil liquefaction, containment of contaminations, manufacture of masonry bricks and blocks (Consoli *et al.* 2010). With the notion that circular economy is the only path that ensures the sustainability of the planet natural resources, a more widespread use of improved soil with hydraulic binders would allow a very relevant contribution to the progressive abandonment of the linear economy model, which still represents about 90% of the world economy (Teixeira *et al.* 2019). Increasing of this technique implementation would also significantly contribute to cost reduction via reusing resources that exist near or at the construction site (Pereira 2021).

The measurement of the mechanical performance of soil-cement is generally carried out by performing UCS and CD tests, as a natural consequence of the accumulated experience with these test procedures applied to concrete (Consoli *et al.* 2010). However, this requires a significant financial and time investment for the preparation of test specimens for laboratory tests, leading to the loss of (at least) several weeks and significant financial resources (Narloch *et al.* 2019). This study aims at demonstrating that artificial neural networks (ANN) can be used to obtain very satisfactory results in UCS and CD prediction of a sandy soil at different ages, and with the use of a reduced number of input parameters (cement and water content, age, w/c, specimen mass, and result of the proctor test of the soil-cement mixture). These parameters are referred as influential in mechanic properties of soil-cement mixtures (Shibazaki 2003, Gazzarrini *et al*. 2005, Tinoco *et al.* 2011, Venda Oliveira *et al.* 2018), and this study comprehends a setup of five different (and common) percentages of cement and water content, which makes its applicability extensive and useful.

An ANN consists of a set of simple interconnected processing elements (units or nodes) whose functionality is

*Corresponding author, Ph.D. Student
E-mail: lfmpereira@student.uc.pt

ISSN: 2005-307X (Print), 2092-6219 (Online)

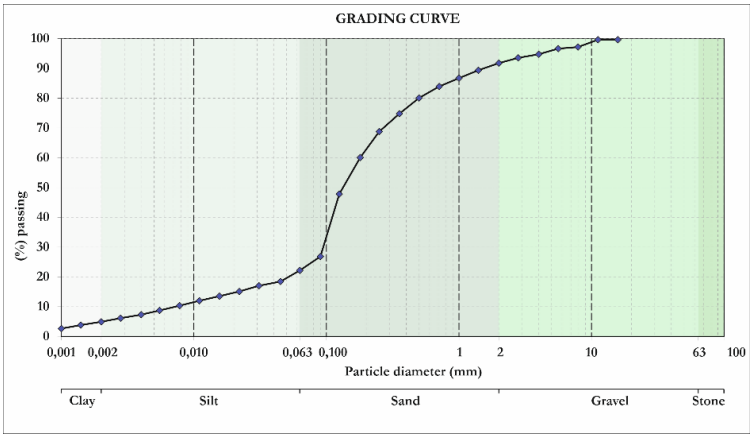

Fig. 1 Particle size distribution curve of the studied Soil (laser granulometer)

inspired by the animal neuron. Its processing capacity resides in the strength of the connections between these units (weighting factors), which are obtained through a process of "learning" from a set of training data (Humphries and Gurney 1997). In the specific case of neural pattern recognition, this process consists of finding similarities and regularities in an automated way, assigning a given input value to a "category". The use of ANN as a forecasting technique has been widely applied in numerous areas of human activity, as an alternative to traditional statistical methods, such as atmospheric sciences (Gardner and Dorling 1998), renewable energies (Kalogirou 2000), polymer composites (Zhang and Friedrich 2003), industrial applications (Meireles *et al.* 2003), in medicine (Lisboa and Taktak 2006), engineering (Waszczyszyn 2011) and geotechnics (Jong *et al.* 2021, Bunawan *et al*. 2018, Bunyamin *et al.* 2018, Armaghani *et al*. 2021). In the specific domain of predicting mechanical parameters in cement-stabilized soils using machine learning methodologies, different methodologies and machine learning algorithms have been applied, with very positive and promising results, in order to predict the UCS of cement-stabilized soils. One may highlight, among others, the works of (Shi *et al*. 2012, Suman *et al*. 2016, Narloch *et al.* 2019, Asteris and Mokos 2020, Tinoco *et al.* 2020, Ngo *et al.* 2021, Pham *et al.* 2021, Zhang *et al*. 2022). Accurate forecast of UCS and CD of a soil-cement using ANN is a matter of extreme relevance as it allows to shorten the time span and cost of a specific work. Additionally, and due to the still limited number of databases available in scientific literature regarding soil-cement, the present work contributes with the publication of (1) a database composed of 150 experimental UCS and CD tests (see Annex A), and (2) results of the application of the neural pattern recognition methodology included in the MATLAB software.

2. Materials, specimen preparation, mechanical test and ANN methodology used

The specimens for the UCS and CD tests were prepared with Portland cement CEM II/B-L 32.5N, and the water used was from the public supply network. The soil was collected in the vicinity of Leiria (Portugal), in an old and deactivated quarry. The particle size analysis conducted in this study was carried out using a Beckman Coulter, model LS230, laser granulometer, according to the recommendations of ISO 13320-1:1999 (ISO 13320-1, 1999), along with the internal procedure of the laboratory. The general preparation of the sample was carried out in accordance with the specification LNEC E 195 (1966) "Dry preparation of samples for identification tests" (LNEC, 1967) .

Fig. 1 shows the particle size distribution curve of the studied soil, obtained by laser granulometer.

Analysing the grading curve, it can be concluded that the soil is composed by 8.5% of gravel-sized particles, 69% of sandy particles, 17% of silt particles and 5.5% of clay-sized particles. The soil was classified as SM – sand with silt, according to ASTM D2487 – 10 (ASTM, 2010). The compaction of the soil-cement specimens followed, in general, the indications foreseen in specification LNEC E 264 – 1972 (LNEC:264, 1972). Fig. 2 shows the different stages of the process of preparing the soil-cement mixture.

A hundred and fifty specimens were prepared with compaction energy equivalent to the Proctor test. Table 1 shows the quantity of specimens prepared for a cement content of 6% (30 specimens), type of test (unconfined compression (UCS) and split tensile test (CD), specimen age when tested (seven days (7D) and twenty-eight days (28D)). In addition to this cement content, specimens with 8%, 10%, 12% and 14% of cement were also prepared, in equal numbers and for the same type of tests and ages.

In Fig. 3, it is possible to observe the compaction curve of the unstabilized soil (identified with "Proctor"), as well as the characteristics of the specimens prepared with different binder percentages (from 6% to 14%). The soil used in the Proctor tests was completely dry at the moment of the preparation of the test specimens, and the water content was determined immediately after the conclusion of the mixture.

It can be concluded that the influence of the binder is great and of paramount importance in the dry density of the soil-cement mixture. UCS tests were performed according to LNEC specification E 264 – 1972 (LNEC:264, 1972),

Fig. 2 (a) soil, (b) soil homogenized with cement, (c) addition of water using a mixer, (d) fresh test specimen, (e) bagged fresh test specimens and (f) portions to determine water content

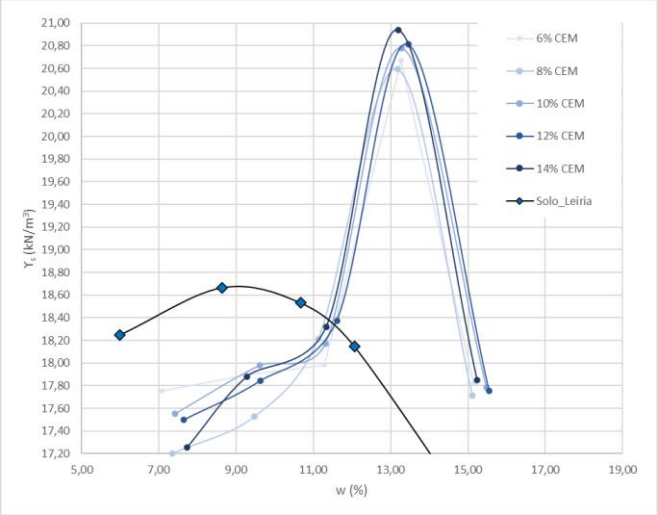

Fig. 3 Compaction curves of the unstabilized soil (light brown) and of the soil-cement mixtures

Table 1 Quantity of test specimens, type of tests and age at the time of the test, for 6% cement content (CEM)

CEM (%)	Water (%)	Type of test and age of the specimen (Nº of specimens)			
		UCS7D	CD7D	UCS28D	CD28D
6	7	1	1	2	2
	9	1	1	2	2
	11	1	1	2	2
	13	1	1	2	2
	15	1	1	2	2

and CD tests were carried out according to NLT 304/89 – "Diametral compressive strength of materials treated with hydraulic binders" (NLT 304-89, 1989). Fig. 4 presents details of the UCS and CD tests.

Fig. 5 presents the results of the UCS and CD tests carried out in this study. The specimen tests at the age of 7 days are represented in orange and with circular symbols.

The specimens tested at the age of 28 days are represented by the blue squares.

The main objective of this study was to achieve a satisfactory forecast of the mechanical parameters UCS and CD of the soil-cement mixtures. A set of six parameters/variables obtained that can be obtained shortly after the preparation of the test specimens were collected

Table 2 Classes with range of values, age and type of test

Test	Age and quantity of tests	Classes	A	B	C	D	E
UCS	7D (25 tests)	Minimum value	2951,87	2328,96	1706,05	1083,14	460,24
		Maximum value	3574,77	2951,87	2328,96	1706,05	1083,14
	28D (50 tests)	Minimum value	5359,56	4202,17	3044,78	1887,39	730,00
		Maximum value	6516,95	5359,56	4202,17	3044,78	1887,39
CD	7D (25 tests)	Minimum value	472,30	372,63	272,97	173,30	73,64
		Maximum value	571,96	472,30	372,63	272,97	173,30
	28D (50 tests)	Minimum value	857,53	672,35	487,16	301,98	116,80
		Maximum value	1042,71	857,53	672,35	487,16	301,98

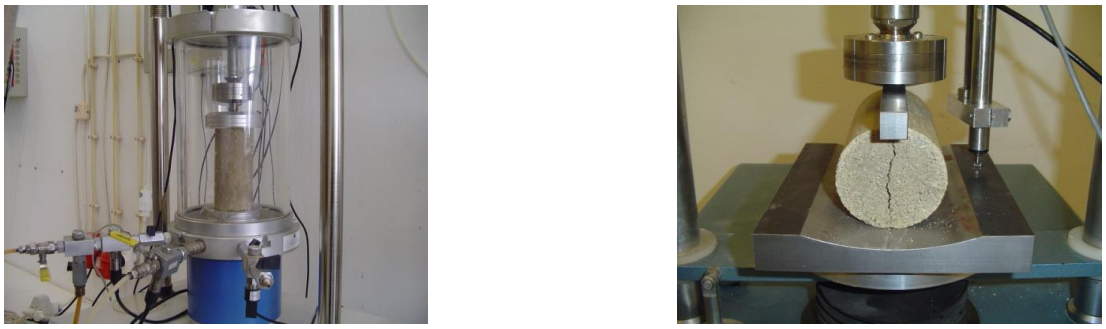

Fig. 4 Details of the UCS test (left), and CD test (right)

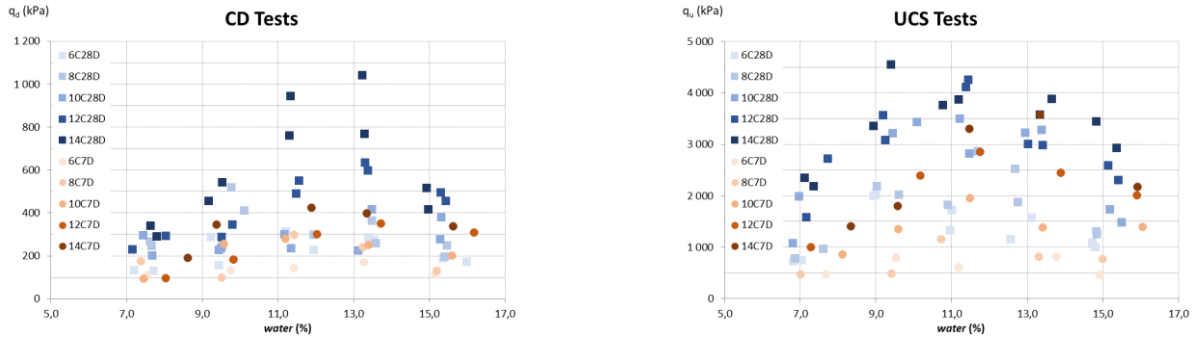

Fig. 5 Results of the UCS (right) and CD tests (left)

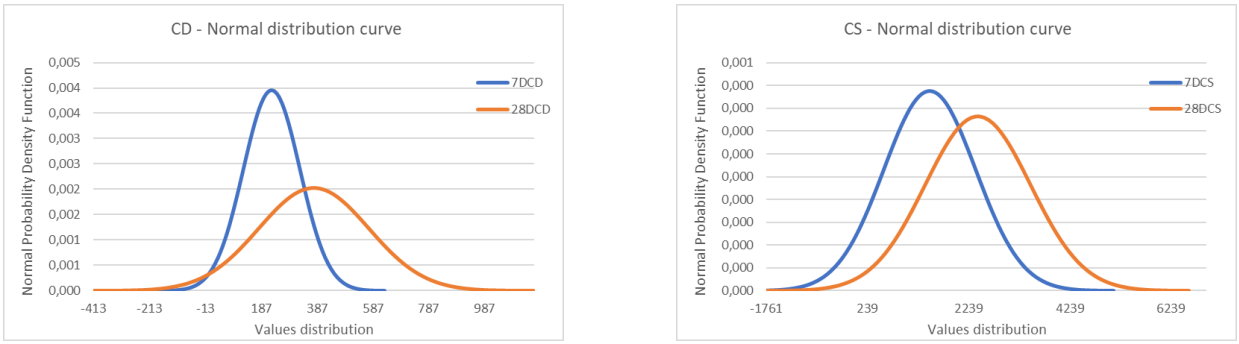

Fig. 6 Normal distribution curve of the CD and UCS results

from a Master's thesis database (Pereira 2021). These input parameters were used to feed the neural network training process in which three MATLAB embedded training functions (*trainbr*, *trainlm* and *trainscg*) were applied. The database was randomly divided into training, validation and testing subsets with a 70:15:15 ratio, respectively, a

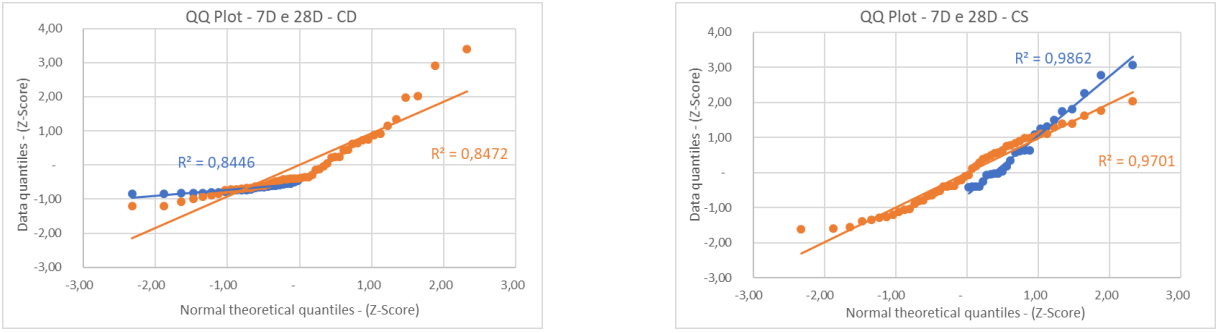

Fig. 7 QQ plots of the CD (left) and UCS tests (right), by age: 7D in blue, and 28D in orange

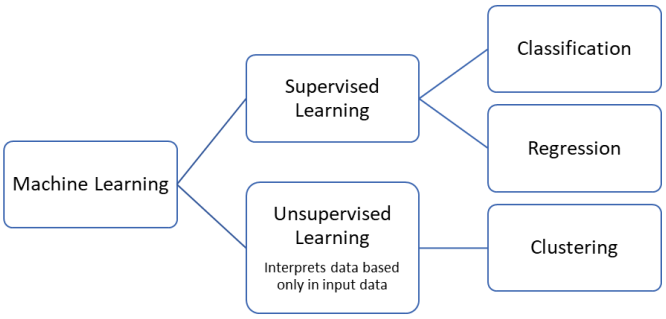

Fig. 8 Categorization flowchart of machine learning

percentage ratio within the range frequently applied in similar studies and established as adequate and efficient (Tinoco *et al.* 2018, Tola *et al*. 2023, Tinoco *et al*. 2011). No parameters integrated more than one group. Each one of these three subsets was composed of input vectors (predictors) in the form of columns of a matrix, and a response vector that indicated the classes in which the input parameters fit.

Table 2 presents the classes defined by the authors, as well as the respective value ranges, organized by age of the specimens, quantity, and type of test.

The statistical analysis of the samples allowed to verify that they present a Gaussian distribution, with the 28 days sample population exhibiting greater variability in both types of test (CD and UCS), when compared to 7 days (see Fig. 6).

This conclusion is supported by the QQ plot presented in Fig. 7, that relates the data and theoretical quantiles (Z-scores) and presents the correlation coefficient (R^2).

The analysis of Fig. 7 allows to verify that the correlation between the data and theoretical Z-scores is very high, being naturally higher in the UCS tests (R^2=0.9862 at 7 days and R^2=0.9701 at 28 days), tests that usually present lower variability than CD tests.

3. Machine learning – supervised learning – classification

Machine learning algorithms find patterns in data, which can improve the assumption of informed decisions and help forecast properties or parameters. Furthermore, these algorithms progressively improve their performance, adapting and "learning" information from these data without the need to base their operation on predetermined equations. A supervised algorithm uses a given set of input and response parameters and trains a model that makes it possible to predict these response parameters in the presence of new input parameters. The supervised learning methodology uses two techniques to train models: regression and classification. Regression technique predicts continuous responses, while classification (the technique used in this study) predicts discrete, categorized responses.

An Artificial Neural Network (ANN) is a mathematical or computational model that mimics the structural and functional aspects of biological neural networks. It consists of an interconnected group of artificial neurons and processes information using a connectionist approach to computation, changing its structure based on a set of information that flows through the network during the learning phase. The neuron is a simple mathematical processing unit that considers one or more inputs and an output. Each input has an associated weight that defines its relative importance, which is then computed by the neuron, resulting an output. This output is modified by an activation (also called transfer) function and forwarded to another neuron, building a feed-forward architecture where the data flows from inputs to outputs, known as multilayer perceptron (MLP) (Flores 2021). In this study, a MLP system was used, composed of two hidden feed-forward layers of neurons (with 20 neurons per layer), with a sigmoid hidden and softmax output activation functions,

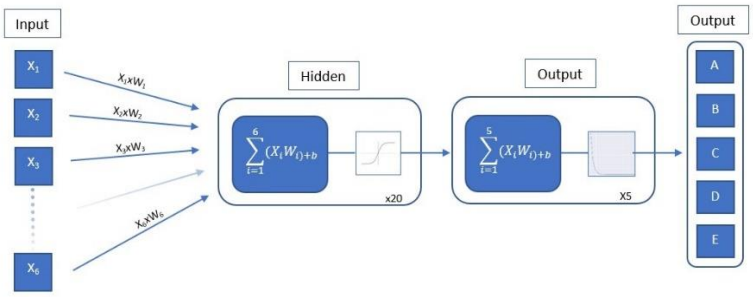

Fig. 9 Diagram of the ANN used

and with scaled conjugate gradient backpropagation. The sigmoid activation function (also called logistic function) was used, since the output to predict was a percentage, and the weighted sum of the input values was set to map values between 0 and 1, through Eq. (1).

$$\sigma(x) = \frac{1}{1 + e^{-x}} \tag{1}$$

where x is the sum of the weighted input values at each neuron.

The softmax activation function is a generalization of the logistic function that converts a vector of numbers into a vector of relative probabilities, and is frequently used as the last transfer function in an ANN on a multi-class classification problem, through Eq. (2)

$$softmax\,(z_i) = \frac{\exp(z_i)}{\Sigma_j \exp(z_j)} \tag{2}$$

where z represents the values from the neurons of the output layer. Later, these values are divided by the sum of exponential values in order to normalize and convert them into probabilities that sum to one. Fig. 9 represents the feed-forward ANN used in the present study.

In Fig. 9, it is possible to see the six inputs parameters, the hidden layer that computes the weighted input values, the sigmoid transfer function that maps all these values into the 0 to 1 interval, the computation of these values in the output layer, and the softmax transfer function that normalizes the values into relative percentages considering five classes. No data was discarded, since none, when carrying out the tests, seemed to be an anomaly or error. Thus, all input and response parameters were considered in the model training.

Several artificial intelligence methodologies have been successfully utilized in geotechnical engineering, particularly in the mechanical characterization of geomaterials, such as artificial neural networks (ANN), Decision Trees (DT), Support Vector Machine (SVM), Genetic Programing (GP), among others (Jong *et al.* 2022).
ANN's are able to compute a mapping from a multivariate space of information to another, can process incomplete data and capture non-linear relationships between the variables of the system. They are "black box" models, which means ANN's do not provide any physical deduction process while analyzing the data (Jong *et al*. 2021).

SVM's perform well in higher dimension, when the number of features are higher, and especially when classes are easily separated linearly, or even non-linearly. On the downside, it can be slow with larger datasets, requiring a large amount of time to process, and it tends to underperform with overlapped classes. It is frequently applied to speech recognition, classification of images, text classification and medical analytics.

DT's does not need to normalize the data, provide easy and intuitive visualization, and the results are not affected by irrelevant features. They can be applied to regression and classification problems, creating a tree like structure developed based on a set of splitting rules. It is a method considered to be prone to overfitting and usually require considerable periods of time to train.

GP's consists of an evolutionary computation methodology that originates a structured representation of the data. It is an extension of genetic algorithms, which are based on natural evolutionary mechanisms such as selection, reproduction, cross-over and mutation, to solve function identification problems (Jong *et al*. 2021).

It is important to emphasize that there are no universal algorithms that can be applied to every situation. Thus, it is crucial that the selection of the training algorithm as well as the input parameters is carried out in an appropriate manner, since it will assume a critical importance in the development of of the machine learning model and its ability to generalize. Likewise, it is important to note that different algorithms can be applied to solve the same problem.

Artificial neural networks are an extremely widespread method in the characterization of soil/rock properties (Abbaszadeh Shahri 2016, Debnath and Dey 2017, Bejarbaneh *et al.* 2018), but other authors applied, with success, different methods to develop efficient models of prediction mechanical properties of materials, like genetic programming (Leong *et al.* 2015), gene-expression programming (Pham *et al*. 2022), support vector machines, k-nearest neighbors, naïve Bayes and random forest (Ren *et al.* 2019), or adaptive neuro-Fuzzy Inference Systems (ANFIS) (Jahed Armaghani *et al.* 2015).
The training functions used in this work are briefly described below.

3.1 Bayesian regularization backpropagation network training function (trainbr)

The initial objective of the network training process is to

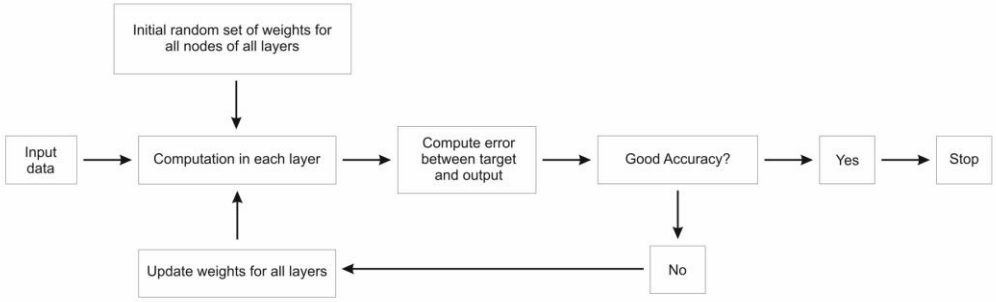

Fig. 10 Flowchart that explains the training of an artificial neural network using the Bayesian backpropagation algorithm

Fig. 11 Confusion matrixes for the CD tests

minimize the sum of squared errors, according to (3).

$$\sigma(x) = \frac{1}{1 + e^{-x}} \tag{3}$$

with ti= target values, and ai=neural network response. The metric "performance" (ED) will be modified to improve the generalization capacity of the neural network. This methodology restricts the dimension of the network's weighting factors, improving its generalization capability, thus being called "regularization". Regularization adds an additional term to the previous equation, becoming the training objective function (4),

$$F = \beta E_D + \alpha E_W \tag{4}$$

where EW is the squared sum of the weights in the network, ED is the squared sum of the residuals between network response values and objective values, and β and α are objective function parameters or hyperparameters. The main difficulty of the regularization process is overcomed by considering these parameters as random variables with specified distributions, considering the relationship between them and unknown variances associated with these specified distributions, thus making it possible to determine the parameters using statistical techniques.

Bayesian regularization backpropagation network algorithm is used with the objective of achieving better generalization and minimal over-fitting in trained datasets of information (networks). The main advantages of this algorithm are that it provides robusts models that reduce or even eliminate the need for lengthy cross-validation, and they are difficult to overtrain, since evidence procedures provide an objective Bayesian criterion for stopping training (Gouravaraju *et al*. 2020, Burden and Winkler 2009).

Bayesian regularization was implemented in MATLAB software *trainbr* function, using by default values of 0 and 1 for α and β, respectively, at the beginning of the training,

Fig. 12 Confusion matrixes for the UCS tests

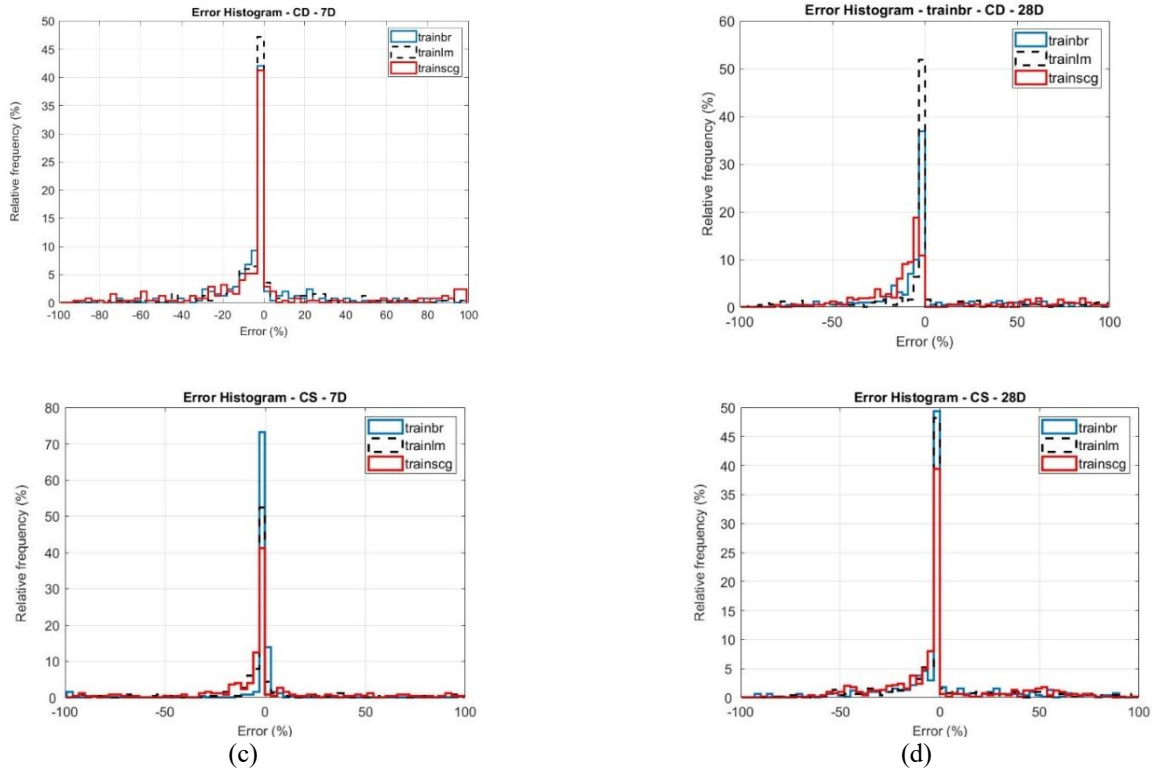

(c) (d)

Fig. 13 Error Histograms for the CD and UCs tests

and continuously improving them by applying the Gauss-Newtonian approximation to the Hessian matrix existing in the Levenberg-Marquardt algorithm, iterating until the point of convergence (Dan Foresee and Hagan 1997).

Fig. 10 illustrates the sequence of steps necessary for training an artificial neural network using the Bayesian backpropagation algorithm.

Analogous to quasi-Newtonian methods, the Levenberg-

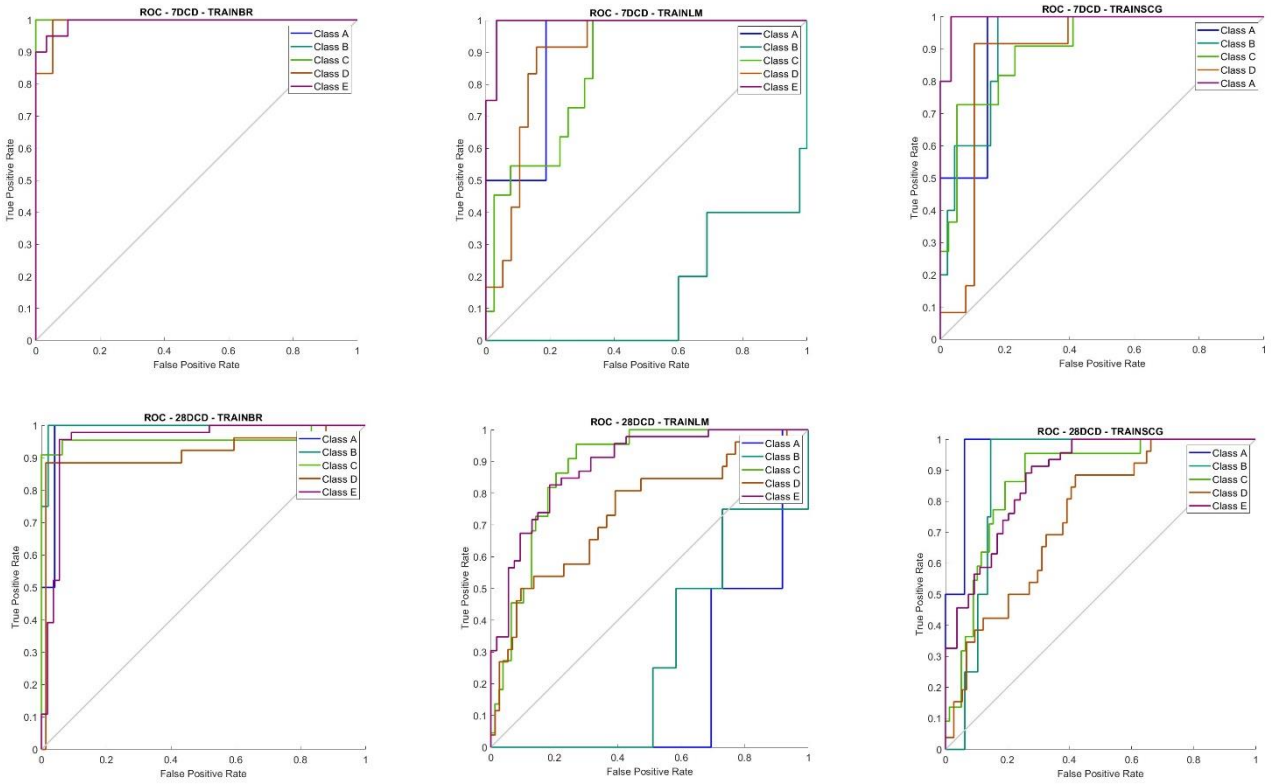

Fig. 14 Receiver Operating Characteristics (ROC) for the CD tests

Marquardt algorithm was conceived to carry out approximations to second-order training speed processes without calculating the Hesse matrix. It is a methodology that proves to be fast and efficient when in a context that the weighting factors (weights) do not exceed a few hundred (Hagan and Menhaj 1994).

3.3 Scaled conjugate gradient backpropagation network training function (trainscg)

The *trainscg* algorithm is a network training function that updates the values of the weighting factors and systematic deviations according to the scaled conjugate gradient method, and it does not perform a line sweep at each iteration (Møller 1993).

4. Results and discussion

The results obtained from the ANN training process (using the three training functions – *trainbr*, *trainlm* and *trainscg*) are presented below. In order to compare the three network training functions results, three evaluation metrics were calculated: the confusion matrix, the error histogram, and the receiver operating characteristics curve (ROC). The confusion matrix is a summary, in percentage accuracy, of the prediction results on classification problem, the error histogram plot returns the errors between the target and predicted values, and the ROC gives the relationship between the ratio of true positive and false positive. Additionally, in the variability study performed (4.1 – Variability study), the RMSE and performance metrics are also used to evaluate the predictive consistency of those training functions. A low value of these metrics means higher predictive power.

The following Figs. 11 to 15 show, for each training function, the results obtained for the UCS and CD tests, at 7 and 28 days of age.

Confusion matrices are “MxM” matrices (with “M” being the number of total target classes) that allows the visualization of the performance of a given machine learning model trained by an algorithm, and they are mainly used for statistical classification, by comparing the real values with the estimated ones by the model, providing ageneral view of how well the model is behaving and what is doing wrong.

As it can be concluded from the previous Figs. 11 and 12, and with respect to the confusion matrices, the forecasted results from the application of the Bayesian regularization backpropagation network training function (*trainbr*) reached percentages of success (when the predicted values matched the actual values) above 90% in below the correct one, with exception for the prediction of the CD and UCS of the specimens with 28 days of age, where, in the case of the CD tests, it classified a total of 48 specimens as class E, when in reality there were only 46. Of these 46 specimens, it classified 44 correctly, and considering 3 others (of actual class D) also as class E, and finally an actual class C as class E. In the case of the UCS tests, the model also considered two specimens as class E, when in reality they were class C and class D. This fact is more visible in the ROC curves, presented bellow (Figs. 14 and 15).

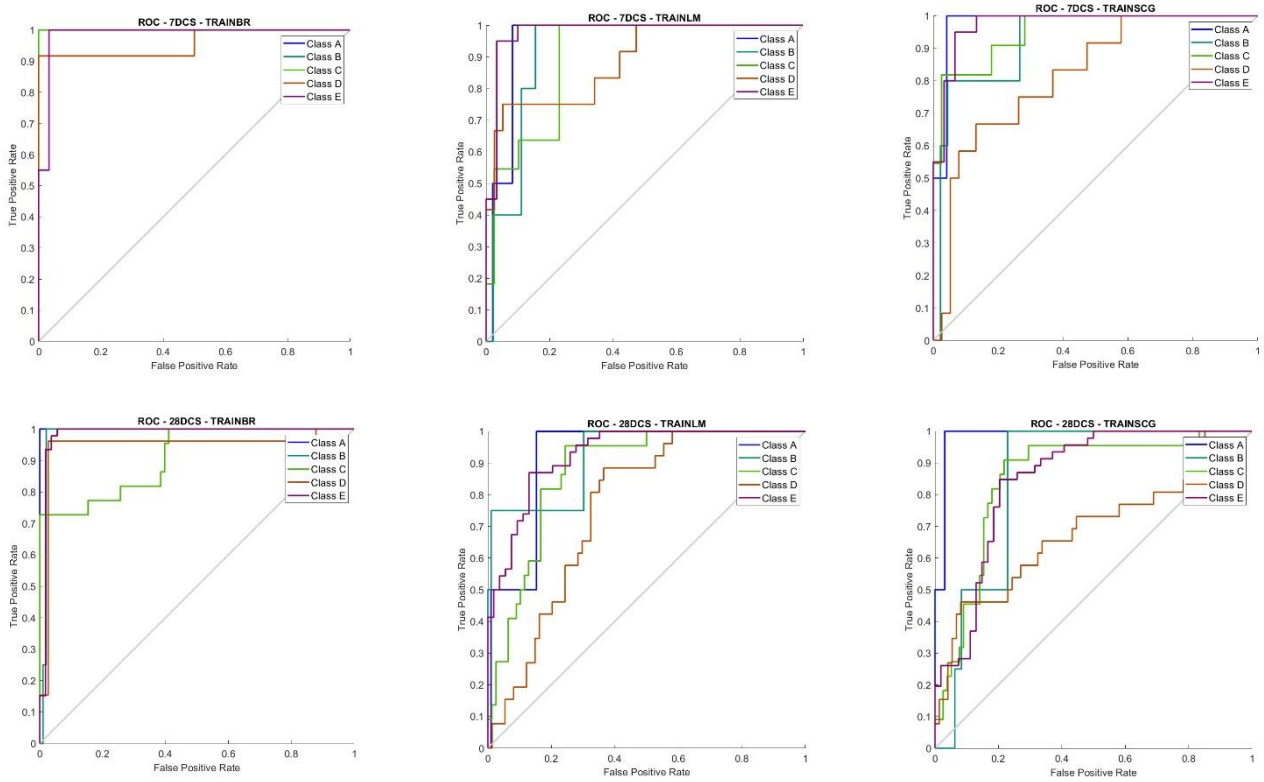

Fig. 15 Receiver Operating Characteristics (ROC) for the UCS tests

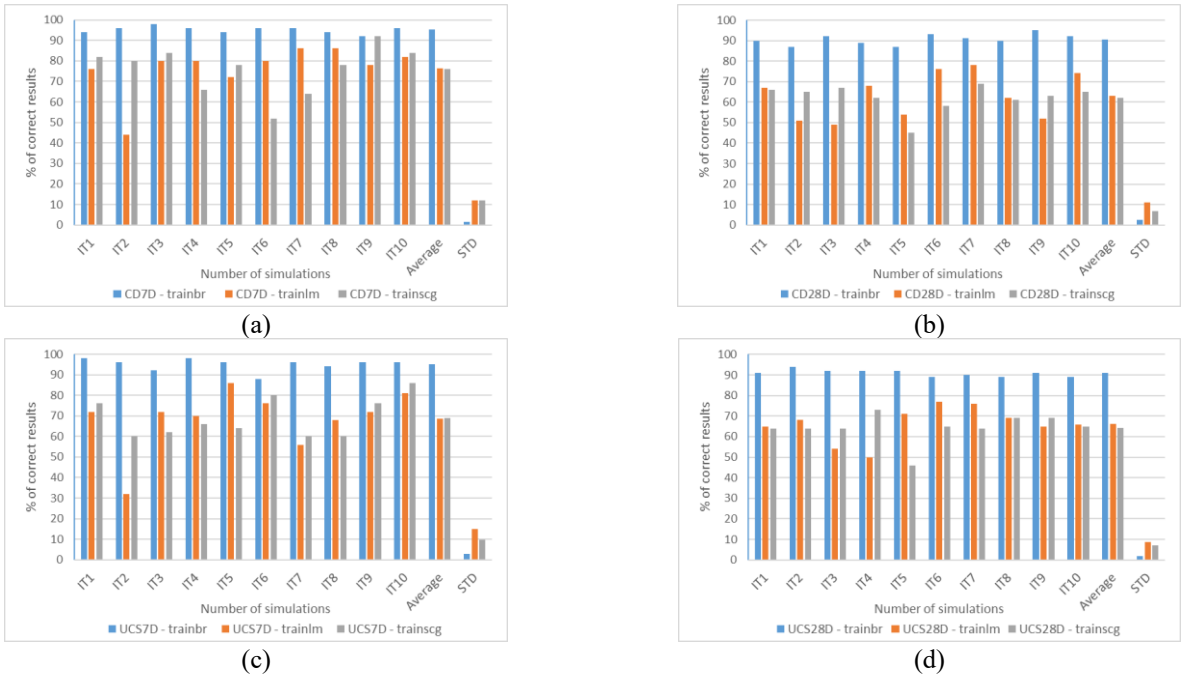

(a) (b)

(c) (d)

Fig. 16 Summary of the 10 overall confusion matrixes results - CD tests: 7D (a), 28D (b), and UCS tests: 7D (c), 28D (d)

The Levenberg-Marquardt and the scaled conjugate gradient backpropagation network training functions (*trainlm* and *trainscg*,) provided significantly less accurate forecasts, being unable to surpass 72% accuracy, making almost a third of the predictions wrong, a percentage that cannot be considered acceptable for the intended purpose.

Additionally, the models trained with these algorithms more often achieved wrong predictions in classes not immediately adjacent to the correct class.

In what concerns the error histogram plots, all the tested training functions displayed an unimodal distribution and performed acceptably, with the highest percentage of errors

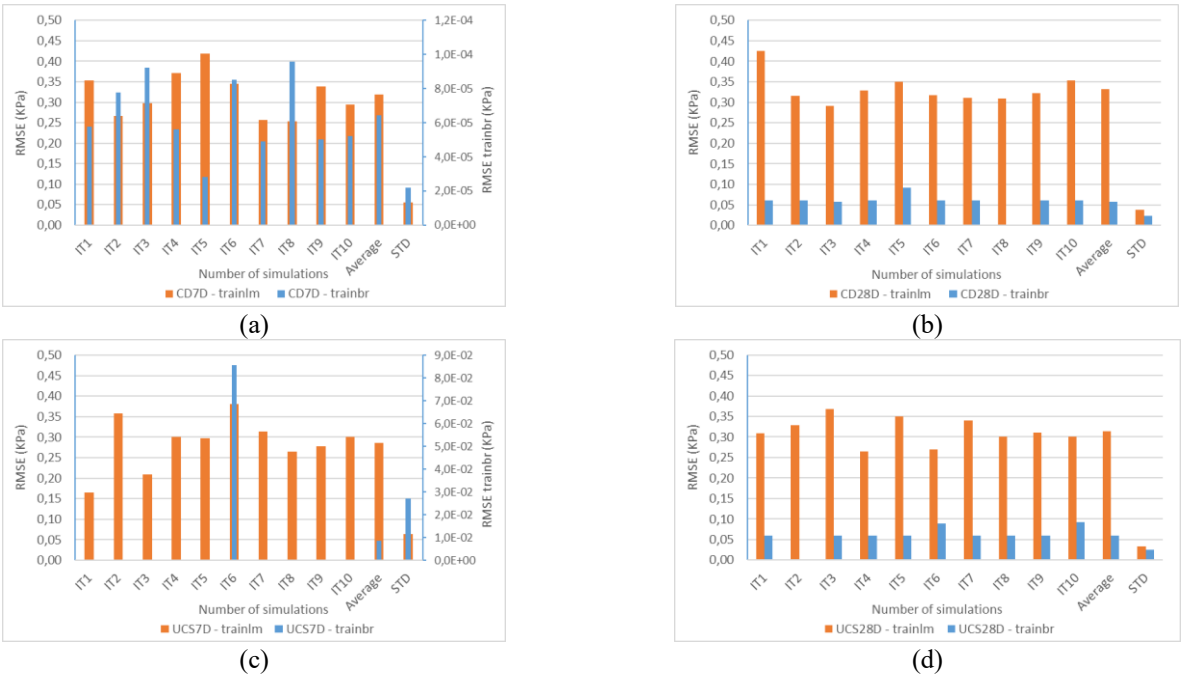

Fig. 17 RMSE of the CD tests, for both tested ages: CD: 7D (a) and 28D (b), and UCS: 7D (c) and 28D (d)

being close to zero, with a mild yet visible tendency to negative values (also visible in the confusion matrices), which indicates that the predicted values were, more often, inferior than the actual values. Error histograms are excellent tools to visualize the dispersion of the population and the values that are more and less common. The error histograms of the *trainbr* (in blue – Fig. 13) shows that the error made by the model centers around zero (deviation from the actual value), and also shows that the dispersion of that error is very low. For instance, the error histograms show, for the *trainbr* algorithm, a probability of the error being very close to the actual value never inferior to 35% (in the case of the 28DCD tests), achieving a probability above 70% in the case of the 7DCS tests. Additionally, the dispersion is considerably inferior to the dispersion obtained from the application of the other algorithms (trainlm and *trainscg*), which also demonstrate a higher probability of errors deviating further from the correct value.

Receiving operating characteristics curves display graphically two parameters of paramount relevance in measuring the performance of a machine learning model, sensitivity and specificity, which are defined as the number of true positive decisions/the number of actually positive cases and the number of true negative decisions/the number of actually negative cases.

Regarding the ROC curves, the ones obtained by the *trainbr* methodology are much more accurate, since the True Positive Rate (TPR, also known as sensitivity) is, for the great majority of thresholds considered in the process of predicting the different classes, one or very close to one, which means that the model almost every time predicts the actual class with an accuracy superior to 90% (there are exceptions, the most visible being the Class C, in the specimens with 28 days of age and subjected to the UCS test, with a prediction accuracy circa 70%), while the False Positive Rate (FPR, also known as 1-specificity) is, also for all the thresholds, zero or close to zero. As for the other two training functions tested (*trainlm* and *trainscg*), the ROC curves reveal a less accurate result, with lower TPR and higher FPR, with the curves being closer to the diagonal grey curve (that indicates an equal percentage of TPR and FPR).

4.1 Variability study

Since the network training procedure splits, by default and in the three network training functions, the dataset in exclusive subsets of training, validation and testing, it was considered appropriate to perform a study of the variability of the results by repeating 10 network training processes.

The objective was to verify if the results of the network training by the different algorithms were “stable” and did not depend on the random division of the dataset in subsets for training, validation and testing. As demonstrated in the Figs. 6 and 7, the dataset presents a Gaussian distribution, with a very high correlation between the data and the theoretical Z-scores. Thus, any considerable difference resulting from the variability study would be due to this random process of division of the dataset and processing by each algorithm. The absence of significant differences demonstrated by the low standard deviation, RMSE and performance metrics prove that the results are credible and reliable.

Results of the 10 repetitions

The results of the performed simulations with the sample population of both test typologies are presented in the next figures (Figs. 16-18), as well as the average and the

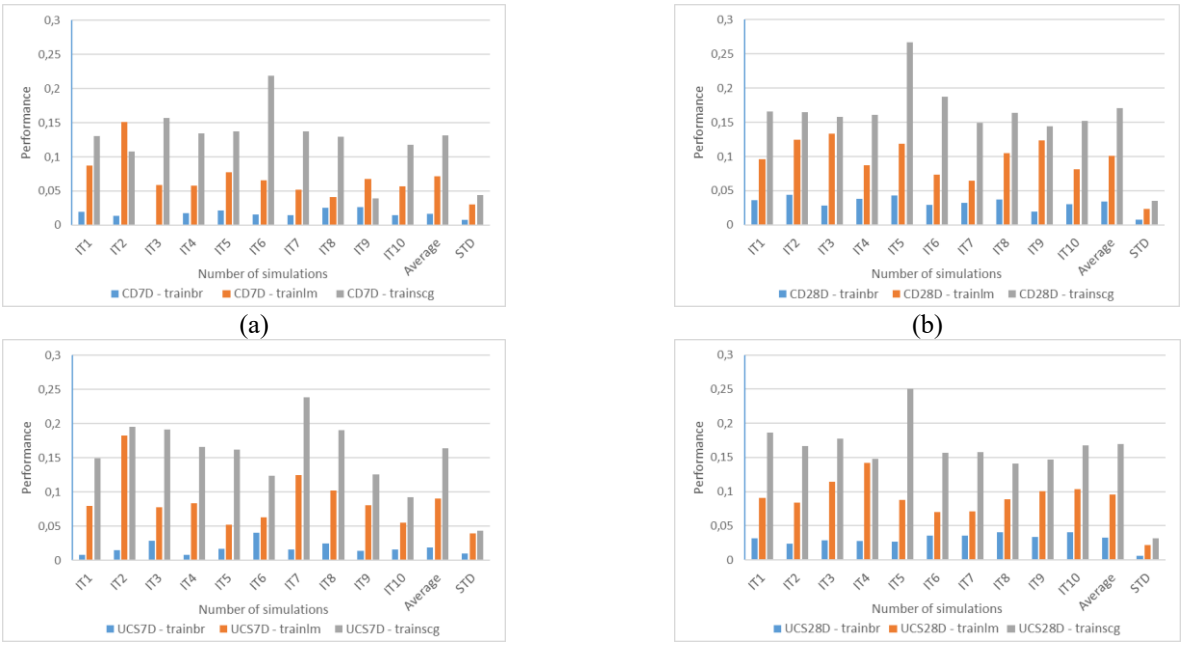

Fig. 18 Results of the metric performance, for the: CD tests - 7D (a) and 28D (b), and UCS tests - 7D (c) and 28D (d)

standard deviation (STD) values.

From the analysis of Fig. 16, it can be concluded that the *trainbr* network training function, in addition to the already mentioned high accuracy percentages (it presents average accuracies of 95,2% and 90,6%, for the ages of 7 and 28 days, respectively), presents a low dispersion in relation to the mean (STD at 7D=1,7%; and at 28D=2,5%), demonstrating to be the most adequate methodology (from the three studied in this work) for this purpose. As for the other training functions (*trainlm* and *trainscg*), they confirmed, in the repetitions carried out, considerably below par results. The *trainlm* network training function achieved percentages of success of 76,4% and 63,1%, for the ages of 7 and 28 days, respectively, with STD values around 11%. Finally, the *trainscg* training function achieved an average percentage of accuracy of 76% and 62,1%, for the ages of 7 and 28 days, respectively, with STD values around 9,4%.

In what concerns the UCS repetitions, it can be concluded that the *trainbr* training function maintains accuracy above 90% (95% at 7 days of age, and 91% at 28 days of age), results that are reinforced with a STD of 3% at 7 days and 1.7% at 28 days, confirming and reinforcing that the *trainbr* algorithm is the methodology that demonstrates better performance of the training algorithms tested in this study.

As for the other training functions (*trainlm* and *trainscg*), they once more confirmed a poorer performance, with accuracies about 25% lower, and with higher STD baselines. The *trainlm* network training function reached percentages of success of 68,5% and 66,1%, for the ages of 7 and 28 days, respectively, with STD values around 11%. Finally, the *trainscg* training function achieved an average percentage of accuracy of 76% and 62,1%, for the ages of 7 and 28 days, respectively, with an average STD of 11,9%.

Finally, the *trainscg* training function reached a percentage of success of 69% and 64,3%, for the ages of 7 and 28 days, respectively, with STD values around 8,4%.

Fig. 17 presents the root mean squared error (RMSE) for both ages tested, for the *trainbr* and *trainlm* training functions.

The *trainbr* training function returned better results also in the RMSE metric, as it can be seen in Figs. 17(a) and 17(c) (secondary axis of the 7-day Figures), being up to 3 orders of magnitude smaller than *trainlm* (represented on the main axis), in the case of the CD tests at 7 days, and up to 2 orders of magnitude smaller, for the case of UCS tests at 7 days. In what concerns the specimens tested at 28 days of age, the differences between the results are smaller, but the *trainbr* algorithm still achieves a better performance, with lower values and lower STD.

Fig. 18 presents the evaluation metric performance, for all the test results.

In the metric performance, and for the case of the CD tests, the *trainbr* function presents values 75% lower than those shown by the *trainlm* function and 87% lower than those achieved by the *trainscg* function, at the age of 7 days, and about 70% lower than the results by the *trainlm* function and 80% lower than those achieved by the function *trainscg*, at the age of 28 days.

In what concerns the UCS tests, the *trainbr* function presents values 80% lower than those exhibited by the *trainlm* function, and 90% lower than those achieved by the *trainscg* function at the age of 7 days, and about 67% lower than the results obtained by the *trainlm* function and 81% lower than those obtained by the function *trainscg* for the age of 28 days.

In all the metrics evaluated in this study, the *trainbr* algorithm demonstrated being the most adequate machine learning methodology to apply in this kind of situations.

5. Conclusions

Application of machine learning algorithms based on input and output parameters (supervised learning) collected from a database composed of one hundred and fifty specimens, aimed at forecasting the output parameters UCS and CD (previously classified into classes) was carried out with a very satisfactory degree of accuracy. The algorithms were applied with resource to only six parameters that are known to be influential, relatively inexpensive and quick to obtain (cement and water content, age of the specimens, w/c ratio, specimen mass and the result of the Proctor test). The *nprtool* (neural pattern recognition) tool implemented in the MATLAB software allowed, using the Bayesian regularization backpropagation network training function, predicting the mechanical performance of soil-cement specimens with accuracy above 90%. The same training function returned the lowest RMSE and performance metrics of all training functions used in this study. The variability study performed showed that it exhibits a reduced STD in both types of tests, which increases the degree of security in the produced forecast.

The results obtained in this study show that the *trainbr* algorithm is better suited for being applied to these kinds of problems, where a set of input and output parameters are used to feed the artificial neural network model, than the *trainlm* and the *trainscg* algorithms. In the opinion of the authors, it validates the robustness for the application of the model to the prediction of these mechanical parameters (UCs and CD) in soil-cement mixtures prepared with sandy soils with similar composition to the one used in this study, as well as with the range of water and cement contents used in this study.

The forecasts obtained are promising and permit, if applied in practice, to save time and resources in the context of ongoing works in a construction site.

Funding

This work was partly financed by FCT / MCTES through national funds (PIDDAC) under the R&D Unit Institute for Sustainability and Innovation in Structural Engineering (ISISE), under reference UIDB / 04029/2020, and under the Associate Laboratory Advanced Production and Intelligent Systems ARISE under reference LA/P/0112/2020.

This work is financed by national funds through FCT - Foundation for Science and Technology, under grant agreement 2022.12096.BD attributed to the 1st author.

Conflicts of Interest

The authors declare no conflicts of interest.

References

Abbaszadeh Shahri, A. (2016), "An optimized artificial neural network structure to predict clay sensitivity in a high landslide prone area using piezocone penetration test (CPTu) data: a case study in southwest of Sweden", *Geotech. Geol. Eng.*, **34**, 745-758.

Armaghani, D.J., Mamou, A., Maraveas, C., Roussis, P.C., Siorikis, V.G., Skentou, A.D. and Asteris, P.G. (2021), "Predicting the unconfined compressive strength of granite using only two non-destructive test indexes", *Geomech. Eng.*, **25**(4), 317-330. https://doi.org/10.12989/gae.2021.25.4.317.

Asteris, P.G. and Mokos, V.G. (2020), "Concrete compressive strength using artificial neural networks", *Neural Comput. Appl.*, **32**(15), 11807-11826. https://doi.org/10.1007/s00521-019-04663-2.

ASTM. (2010), Standard practice for classification of soils for engineering purposes, Unified Soil Classification System (D2487-06). ASTM International, 06.

Bejarbaneh, B.Y., Bejarbaneh, E.Y., Amin, M.F.M., Fahimifar, A., Jahed Armaghani, D. and Majid, M.Z.A. (2018), "Intelligent modelling of sandstone deformation behaviour using fuzzy logic and neural network systems", *Bull. Eng. Geol. Environ.*, **77**, 345-361. https://doi.org/10.1007/s10064-016-0983-2.

Bunawan, A.R., Momeni, E., Armaghani, D.J., Nissa binti Mat Said, K. and Rashid, A.S.A. (2018), "Experimental and intelligent techniques to estimate bearing capacity of cohesive soft soils reinforced with soil-cement columns", *Measurement: J. Int. Measurement Confederation*, **124**, 529-538. https://doi.org/10.1016/j.measurement.2018.04.057.

Bunyamin, S.A., Ijimdiya, T S., Eberemu, A.O. and Osinubi, K.J. (2018), "Artificial neural networks prediction of compaction characteristics of black cotton soil stabilized with cement kiln dust", *J. Soft Comput. Civil Eng.*, **2**(3), 50-71.

Burden, F. and Winkler, D. (2009), "Bayesian regularization of neural networks", *Artif. Neural Networks: Method. Appl.*, 23-42.

Consoli, N.C., Cruz, R.C., Floss, M.F. and Festugato, L. (2010), "Parameters controlling tensile and compressive strength of artificially cemented sand", *J. Geotech. Geoenviron. Eng.*, **136**(5), 759-763. https://doi.org/10.1061/(asce)gt.1943-5606.0000278.

Correia, A.A.S., Venda Oliveira, P.J. and Lemos, L.J.L. (2013), "Prediction of the unconfined compressive strength in soft soil chemically stabilized", *Proceedings of the 18th International Conference on Soil Mechanics and Geotechnical Engineering: Challenges and Innovations in Geotechnics,* ICSMGE 2013.

Dan Foresee, F. and Hagan, M.T. (1997), "Gauss-Newton approximation to bayesian learning", *IEEE International Conference on Neural Networks - Conference Proceedings*, *3*, 1930-1935. https://doi.org/10.1109/ICNN.1997.614194

Debnath, P. and Dey, A.K. (2017), "Prediction of laboratory peak shear stress along the cohesive soil–geosynthetic interface using artificial neural network", *Geotech. Geol. Eng.*, **35**, 445-461.

Erzín, Y. and Gul, T.O. (2013), "The use of neural networks for the prediction of the settlement of pad footings on cohesionless soils based on standard penetration test", *Geomech. Eng.*, **5**(6), 541-564. https://doi.org/10.12989/gae.2013.5.6.541.

Flores, J.A. (2021), Focus on artificial neural networks. In *Focus on Artificial Neural Networks*. Nova Science Publishers.

Gazzarrini, P., Kokan, M. and Jungaro, S. (2005), "Case History of Jet-Grouting in British Columbia. Underpinning of CN Rail Tunnel in North Vancouver", *Geoteh. News -Vancouver*, **23**(4), 47.

Gouravaraju, S., Narayan, J., Sauer, R.A. and Gautam, S.S. (2020), A bayesian regularization-backpropagation neural network model for peeling computations. arXiv 2020. *ArXiv Preprint ArXiv:2006.16409*.

Hagan, M.T. and Menhaj, M.B. (1994), "Training feedforward networks with the marquardt algorithm", *IEEE T. Neural Networ.*, **5**(6), 989-993. https://doi.org/10.1109/72.329697

Humphries, M.D. and Gurney, K.N. (1997), *An introduction to*

neural networks (Routledge (Ed.)).
ISO 13320-1. (1999), *Particle Size Analysis–Laser Diffraction Methods–Part 1: General Principles*.
Jahed Armaghani, D., Tonnizam Mohamad, E., Momeni, E., Narayanasamy, M.S. and Mohd Amin, M.F. (2015), "An adaptive neuro-fuzzy inference system for predicting unconfined compressive strength and Young's modulus: a study on Main Range granite", *Bull. Eng. Geol. Environ.*, **74**(4), 1301-1319. https://doi.org/10.1007/s10064-014-0687-4.
Javadi, A.A. and Rezania, M. (2009), "Applications of artificial intelligence and data mining techniques in soil modeling", *Geomech. Eng.*, **1**(1), 53-74. https://doi.org/10.12989/gae.2009.1.1.053.
Jong, S.C., Ong, D.E.L. and Oh, E. (2021), "State-of-the-art review of geotechnical-driven artificial intelligence techniques in underground soil-structure interaction", *Tunn. Undergr. Sp. Tech.*, 113. https://doi.org/10.1016/j.tust.2021.103946.
Jong, S.C., Ong, D.E.L. and Oh, E. (2022), "A novel Bayesian inference method for predicting optimum strength gain in sustainable geomaterials for greener construction", *Constr. Build. Mater.*, **344**. https://doi.org/10.1016/j.conbuildmat.2022.128255.
Kalogirou, S.A. (2000), "Artificial neural networks in renewable energy systems applications: A review", *Renew. Sust. Energ. Rev.*, **5**(4), 373-401. https://doi.org/10.1016/S1364-0321(01)00006-5.
Leong, H.Y., Ong, D.E.L., Sanjayan, J.G. and Nazari, A. (2015), "A genetic programming predictive model for parametric study of factors affecting strength of geopolymers", *RSC Advances*, **5**(104), 85630-85639.
Lisboa, P.J. and Taktak, A.F.G. (2006), "The use of artificial neural networks in decision support in cancer: A systematic review", *Neural Networks*, **19**(4), 408-415. https://doi.org/10.1016/j.neunet.2005.10.007.
LNEC:264. (1972), *Solo-cimento - ensaio de compressão*.
LNEC. (1967), *Documentação normativa Especificação do LNEC E 195-1966: Solos - Preparação por via seca de amostras para ensaios de identificação*.
Luat, N.V., Lee, K. and Thai, D.K. (2020), "Application of artificial neural networks in settlement prediction of shallow foundations on sandy soils", *Geomech. Eng.*, **20**(5), 385-397. https://doi.org/10.12989/gae.2020.20.5.385.
Meireles, M.R.G., Almeida, P.E.M. and Simões, M.G. (2003), "A comprehensive review for industrial applicability of artificial neural networks", *IEEE T. Ind. Electron.*, **50**(3), 585-601. https://doi.org/10.1109/TIE.2003.812470.
Møller, M.F. (1993), "A scaled conjugate gradient algorithm for fast supervised learning", *Neural Networks*, **6**(4), 525-533. https://doi.org/10.1016/S0893-6080(05)80056-5.
Narloch, P., Hassanat, A., Tarawneh, A.S., Anysz, H., Kotowski, J., and Almohammadi, K. (2019), "Predicting compressive strength of cement-stabilized rammed earth based on SEM images using computer vision and deep learning", *Appl. Sci*., **9**(23), 5131. https://doi.org/10.3390/app9235131.
Ngo, H.T.T., Pham, T.A., Vu, H.L.T. and Van Giap, L. (2021), "Application of artificial intelligence to determined unconfined compressive strength of cement-stabilized soil in Vietnam", *Appl. Sci*., **11**(4), 1-20. https://doi.org/10.3390/app11041949.
NLT 304-89. (1989), *NLT-304-89. Diametral compressive strength of materials treated with hydraulic binders*.
Pereira, L.F.M. (2021), *Estudo do comportamento mecânico de dois solos estabilizados com cimento*. Universidade de Coimbra.
Pham, V.N., Oh, E. and Ong, D.E.L. (2022), "Effects of binder types and other significant variables on the unconfined compressive strength of chemical-stabilized clayey soil using gene-expression programming", *Neural Comput. Appl.*, **34**(11), 9103-9121. https://doi.org/10.1007/s00521-022-06931-0.
Pham, V.N., Do, H.D., Oh, E. and Ong, D.E.L. (2021), "Prediction of unconfined compressive strength of cement-stabilized sandy soil in Vietnam using artificial neural networks (ANNs) model", *Int. J. Geotech. Eng.*, **15**(9), 1177-1187. https://doi.org/10.1080/19386362.2020.1862539.
Ren, Q., Wang, G., Li, M. and Han, S. (2019), "Prediction of rock compressive strength using machine learning algorithms based on spectrum analysis of geological hammer", *Geotech. Geol. Eng.*, **37**(1), 475-489. https://doi.org/10.1007/s10706-018-0624-6.
Shi, X., Liu, Q. and Xiujuan, L. (2012), "Application of SVM in predicting the strength of cement stabilized soil", *Appl. Mech. Mater.*, **160**, 313-317. https://doi.org/10.4028/www.scientific.net/AMM.160.313.
Shibazaki, M. (2003), State of practice of jet grouting. In *Grouting and Ground Treatment*.
Suman, S., Mahamaya, M. and Das, S.K. (2016), "Prediction of maximum dry density and unconfined compressive strength of cement stabilised soil using artificial intelligence techniques", *Int. J. Geosynth. Ground Eng.*, **2**(2), 1-11. https://doi.org/10.1007/s40891-016-0051-9.
Teixeira, J.P., Pereira, M. and Teixeira, J.A. (2019), *Circular Economy in the Civil Construction Sector I*. Lisbon and Tagus Valley Regional Coordination and Development Commission.
Tinoco, J., Alberto, A., da Venda, P., Gomes Correia, A. and Lemos, L. (2020), "A novel approach based on soft computing techniques for unconfined compression strength prediction of soil cement mixtures", *Neural Comput. Appl.*, **32**(13), 8985-8991. https://doi.org/10.1007/s00521-019-04399-z.
Tinoco, J., Correia, A.G. and Cortez, P. (2011), "Application of data mining techniques in the estimation of the uniaxial compressive strength of jet grouting columns over time", *Constr. Build. Mater.*, **25**(3), 1257-1262. https://doi.org/10.1016/j.conbuildmat.2010.09.027.
Tinoco, J., Gomes Correia, A., Cortez, P. and Toll, D.G. (2018), "Data-driven model for stability condition prediction of soil embankments based on visual data features", *J. Comput. Civil Eng.*, **32**(4), 4018027.
Tola, S., Tinoco, J., Matos, J.C. and Obrien, E. (2023), "Scour detection with monitoring methods and machine learning algorithms - A critical review", *Appl. Sci.*, **13**(3), 1661.
Venda Oliveira, P.J., Correia, A.A.S. and Cajada, J.C.A. (2018), "Effect of the type of soil on the cyclic behaviour of chemically stabilised soils unreinforced and reinforced with polypropylene fibres", *Soil Dyn. Earthq. Eng.*, **115**, 336-343. https://doi.org/10.1016/j.soildyn.2018.09.005.
Wang, L. (2002), Cementitious Stabilization of Soils in the Presence of Sulfate. In *Journal of Chemical Information and Modeling*. Louisiana State University and Agricultural & Mechanical College.
Waszczyszyn, Z. (2011). "Artificial neural networks in civil engineering: Another five years of research in Poland", *Comput .Assisted Mech. Eng. Sci.*, **18**(3), 131-146. https://cames.ippt.pan.pl/index.php/cames/article/view/110.
Zhang, G., Chen, C., Zhang, Y., Zhao, H., Wang, Y. and Wang, X. (2022), "Optimised neural network prediction of interface bond strength for GFRP tendon reinforced cemented soil", *Geomech. Eng.*, **28**(6), 599-611. https://doi.org/10.12989/gae.2022.28.6.599.
Zhang, Z. and Friedrich, K. (2003), "Artificial neural networks applied to polymer composites: A review", *Compos. Sci. Tech.*, **63**(14), 2029-2044. https://doi.org/10.1016/S0266-3538(03)00106-4.

CC